PHYSICAL REVIEW B **90**, 081106(R) (2014)

Spectroscopy and dynamics of unoccupied electronic states of the topological insulators Sb_2Te_3 and Sb_2Te_2S

J. Reimann,[1] J. Güdde,[1,*] K. Kuroda,[1] E. V. Chulkov,[2,3] and U. Höfer[1]

[1]*Fachbereich Physik und Zentrum für Materialwissenschaften, Philipps-Universität, 35032 Marburg, Germany*

[2]*Donostia International Physics Center (DIPC), 20018 San Sebastián, Spain*

[3]*Departamento de Física de Materiales UPV/EHU, Centro de Física de Materiales CFM - MPC and Centro Mixto CSIC-UPV/EHU, 20080 San Sebastián/Donostia, Basque Country, Spain*

(Received 3 June 2014; revised manuscript received 18 July 2014; published 13 August 2014)

Time- and angle-resolved two-photon photoemission (2PPE) was used to study the electronic structure and ultrafast electron dynamics of the *p*-doped topological insulator Sb_2Te_3 and its derivative Sb_2Te_2S. Our 2PPE experiments directly reveal that the massless Dirac-cone like energy dispersion of topological surface states is realized above the Fermi energy in both materials. The observed bulk conduction bands of Sb_2Te_2S are found to be shifted to higher energies as compared to Sb_2Te_3. This shift has, however, surprisingly almost no influence on the electron dynamics in the topological surface state, which proceed on a picosecond time scale.

DOI: 10.1103/PhysRevB.90.081106 PACS number(s): 73.20.−r, 78.47.J−, 79.60.Bm

Three-dimensional topological insulators have attracted a lot of attention due to the unique transport properties of electrons in the topological surface state (TSS), which are directly related to its spin texture and Dirac-cone-like energy dispersion [1]. Particularly promising materials of this class are Sb_2Te_3 and derivatives. The study of magnetic coupling, e.g., is most progressed in magnetic doped Sb_2Te_3 compounds, which finally resulted in the observation of the anomalous quantum Hall effect [2]. Moreover, it has been suggested that the substitution of the central Te layer in the quintuple layers of Sb_2Te_3 by S considerably increases the band gap and shifts the Dirac point above the valence-band maximum into the bulk band gap [3,4]. In this way, Sb_2Te_2S is expected to attain a number of specific advantages in terms of transport properties. Despite the importance of these compounds, experimental investigations of their electronic structure are scarce. So far, the presence of a massless energy dispersion of the TSS could be only concluded from Landau-level spectroscopy of Sb_2Te_3 thin films [5]. The reason for this lack of spectroscopic data is substitutional Sb defects at Te sites [6], which result in *p* doping of Sb_2Te_3. This makes it difficult to perform direct band mapping of the TSS by angle-resolved photoelectron spectroscopy (ARPES) [7,8], unlike for the widely studied Bi_2Se_3, which has the same tetradymitelike crystal structure as Sb_2Te_3 but is found to be *n* doped.

In this Rapid Communication, we present a study of the electronic structure and ultrafast electron dynamics of Sb_2Te_3 and Sb_2Te_2S by two-photon photoemission (2PPE), a combination of ARPES with laser pump-probe techniques [9]. Because this technique uses short pump pulses to populate initially unoccupied states before the excited electrons are photoemitted by time-delayed probe pulses, it is particularly well suited for the investigation of *p*-doped topological insulators. It can not only explore the electronic structure above the Fermi energy, but makes it also possible to study the dynamics of excited electrons in the TSS directly in the time domain [9–15]. Our 2PPE experiments unambiguously show that Sb_2Te_3 and Sb_2Te_2S both possess a TSS with a Dirac-cone-like energy dispersion above the Fermi energy. In agreement with theoretical predictions, we find that the unoccupied bulk bands of Sb_2Te_2S are shifted to higher energies as compared to Sb_2Te_3. This shift has, however, surprisingly almost no influence on the coupling between the TSS and the bulk bands.

The experiments were carried out in a μ-metal shielded UHV chamber at a base pressure of 3×10^{-11} mbar. The optical setup is described in detail in Ref. [16]. It is based on a 250-kHz laser system that provides tunable laser pulses in the visible range with a typical photon energy of 2.58 eV and a pulse length of 50 fs. One part of these pulses was used as visible pump pulses (50 nJ/pulse) with variable time delay, while the other part was frequency doubled to provide ultraviolet probe pulses (80 fs, 0.5 nJ/pulse). The *p*-polarized light was focused onto the sample at an angle of incidence of 78° into a spot with a diameter of 100 μm. Photoelectrons were detected by a hemispherical analyzer (Specs Phoibos 150) with a display-type detector. The angular dispersion was measured within the plane of light incidence. The photon energy of the pump pulses (5.15 eV) was matched to the work function of the samples in order to reduce the background due to one-photon photoemission. Single-crystal Sb_2Te_3 and Sb_2Te_2S samples were cleaved *in situ* by the Scotch tape method at a pressure of 3×10^{-10} mbar followed by a rapid recovery back to the base pressure within a minute. On the one hand, this procedure ensures minimal surface contaminations, on the other hand, we find that both, Sb_2Te_3 and Sb_2Te_2S, are astonishingly insensitive to the exposure of residual gases [17]. Most data shown here were acquired at room temperature.

Figures 1(d) and 1(e) give an overview of the 2PPE spectra of Sb_2Te_3 and Sb_2Te_2S. These data have been acquired for temporal overlapping pump and probe pulses where all bands can be observed simultaneously. Both materials show similar spectral structures which will be discussed in the following from low to high energies.

The high intensity close above the Fermi energy E_F is assigned to the transiently populated valence band (VB), which overlaps with the lower branch of the topological

*Jens.Guedde@physik.uni-marburg.de

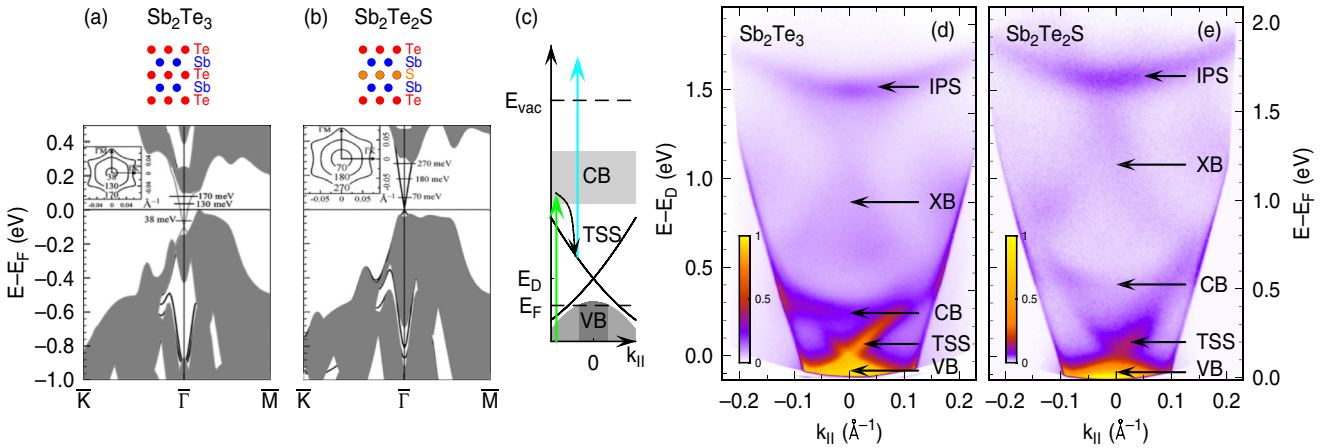

FIG. 1. (Color online) (a) and (b) Calculated band structure together with the stacking order of Te, Sb, and S atoms in the quintuple layers of Sb_2Te_3 and Sb_2Te_2S, respectively (taken with permission from Ref. [3]). Shaded areas show the surface-projected bulk bands, lines indicate the topological surface state. (c) Excitation scheme for the population of the TSS with visible pump pulses via transfer from the bulk conduction band and subsequent photoemission with ultraviolet probe pulses. (d) and (e) Angle-resolved 2PPE spectra for temporal overlapping pump and probe pulses of Sb_2Te_3 and Sb_2Te_2S, respectively. The arrows indicate the top of the valence band (VB), the topological surface state (TSS), the bulk conduction band (CB), higher bulk and surface bands (XB), and the first image potential state (IPS).

surface state (TSS). Both samples are found to be p-doped with E_F being close below the top of the VB at $\bar{\Gamma}$. In the 2PPE spectra shown in Figs. 1(d) and 1(e), the energy of the Dirac point E_D is located at $E_D - E_F = 135(20)$ meV and 120(20) meV, respectively. These values vary within ±50 meV for different preparations, which we attribute to a varying density of surface defects. For this reason, we give in the following all energies with respect to E_D rather than to E_F. A considerable population of the TSS can be observed for energies above E_D of ∼350 meV for Sb_2Te_3. For Sb_2Te_2S, it extends up to 500 meV. It is evident that the 2PPE data for both materials show a pronounced asymmetry in the emission from the TSS with the intensity for negative values of $k_\parallel$ being strongly suppressed. Such asymmetric intensity distribution has been also observed in ARPES spectra of Bi_2Se_3 and has been explained by an interference effect in the photoemission process [18].

The main difference between the spectra of Sb_2Te_3 and Sb_2Te_2S is related to the energy position of the TSS with respect to the higher-lying bands. In agreement with the theoretical calculations [Figs. 1(a) and 1(b)], we observe an upshift of these bands for Sb_2Te_2S as compared to Sb_2Te_3. This can be already concluded from the position of the conduction band (CB), which we identify as the parabolic band close above the TSS. It is more pronounced for Sb_2Te_3 where its minimum is ∼250 meV above E_D. For Sb_2Te_2S, the position of the minimum is shifted towards a higher energy by at least 100 meV. The determination of the actual position of the conduction-band minimum (CBM) with a single probe photon energy is, however, not unambiguous due to the k_z dependence of the photoemission intensity [19], but the upshift of the bands can be also clearly seen by comparing the faint X-shaped structures (XB), which we assign to higher-lying bulk and surface bands. The parabolic band above $E - E_F = 1.5$ eV stems from the first ($n = 1$) image-potential state (IPS), which is only apparently located at this low energy because the roles of pump and probe pulses are interchanged [20].

Figure 2 presents the high-resolution 2PPE data of the TSS of Sb_2Te_3 and Sb_2Te_2S for a comparison with the calculated surface band structure of Ref. [3]. The data of Sb_2Te_3 show an excellent agreement with the theory for the dispersion along the $\bar{\Gamma}$-$\bar{K}$ direction (solid lines) [Fig. 2(a)]. For other sample orientations we find some indications of the predicted dispersion asymmetry between $\bar{\Gamma} - \bar{M}$ and $\bar{\Gamma} - \bar{K}$ directions, the so-called warping [1]. For Sb_2Te_2S, theory predicts a much less pronounced warping as compared to Sb_2Te_3 [Fig. 2(b)]. Our data for the TSS of Sb_2Te_2S agree very well with the calculations including details such as a stronger flattening of the lower branch of the surface state below E_D as compared to Sb_2Te_3.

One remarkable difference between the spectra of Sb_2Te_3 and Sb_2Te_2S is related to the form of the dispersion of the TSS. In all of our data, Sb_2Te_3 shows a straight linear dispersion with a Fermi velocity of $v_F = 2.5(0.2)\times10^5$ m/s [21]. The

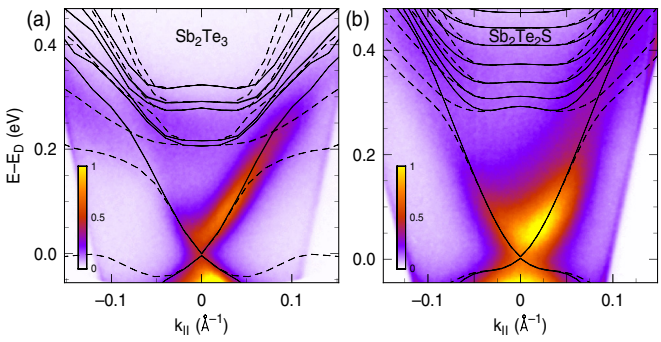

FIG. 2. (Color online) Angle-resolved 2PPE spectra of Sb_2Te_3 along $\bar{\Gamma}$-$\bar{K}$ (a) and of Sb_2Te_2S along a direction in between $\bar{\Gamma}$-$\bar{K}$ and $\bar{\Gamma}$-$\bar{M}$ (b) for the energy region of the TSS at a pump-probe delay of 670 and 870 fs for Sb_2Te_3 and Sb_2Te_2S, respectively. The lines show the calculated surface band structure of Ref. [3] along $\bar{\Gamma}$-$\bar{K}$ (solid lines) and $\bar{\Gamma}$-$\bar{M}$ (dashed lines).

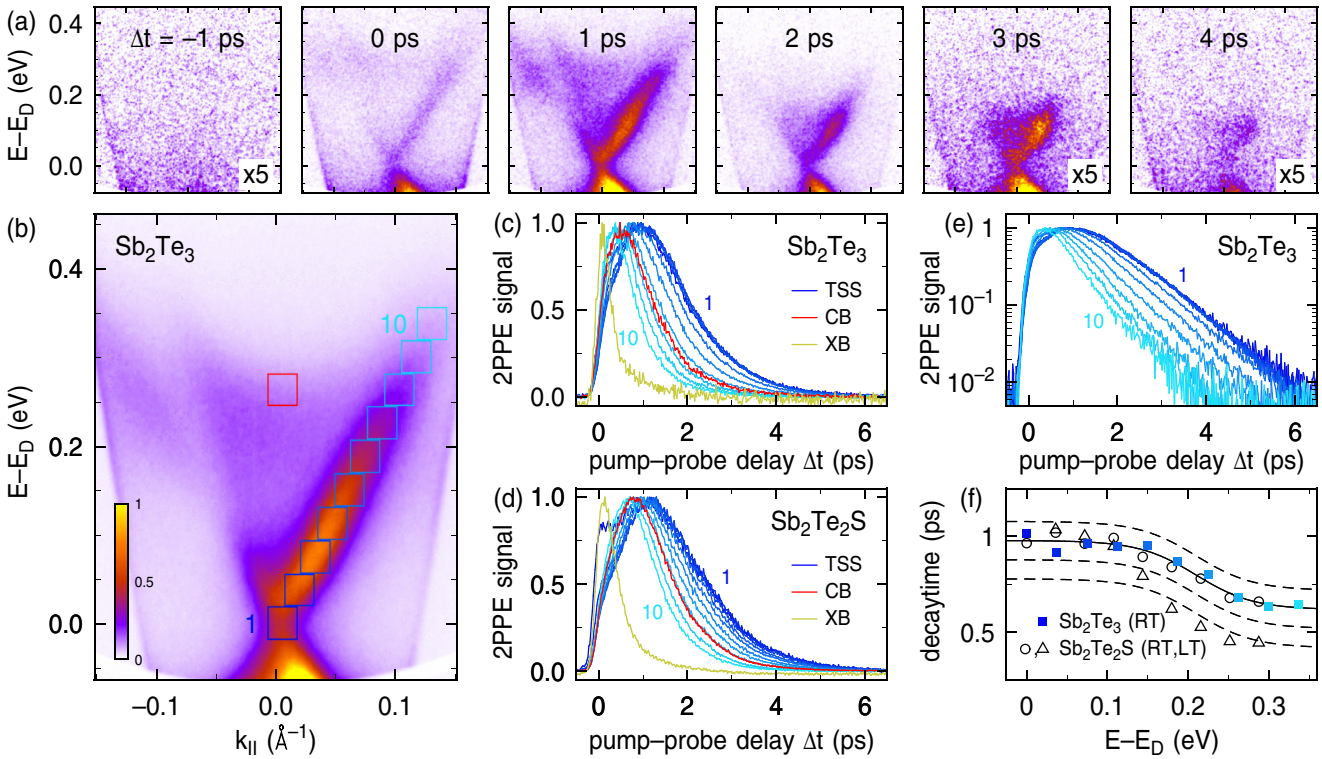

FIG. 3. (Color online) (a) Snapshots of the 2PPE spectra of Sb_2Te_3 for selected pump-probe delays Δt. The intensity for $\Delta t = -1$, 3, and 4 ps is enhanced by a factor of 5. (b) 2PPE data of Sb_2Te_3 (compare Fig. 2(a)) with rectangles that indicate the integration windows for the transient 2PPE intensities. (c) Transient 2PPE intensities for Sb_2Te_3 within the integration windows shown in (b). The curve for XB corresponds to a window at $E - E_D = 650$ meV. All data are normalized to their respective maximum. (d) Transients for Sb_2Te_2S within corresponding windows at the same energies above E_D. (e) Logarithmic plot of the data in (c) for the TSS. (f) Decay times of the 2PPE intensity along the TSS for Sb_2Te_3 at room temperature (RT; filled blue squares) and for Sb_2Te_2S at room temperature (RT; open dots) and at 40 K (LT; open triangles). The solid line is a guide to the eye. The dashed lines indicate the variation of the decay times for different preparations at room temperature.

data for Sb_2Te_2S, on the other hand, clearly show a finite curvature close to E_D. Such deviation from a strict linear dispersion is also visible in ARPES data of other multinary compounds [22,23]. Its origin is, however, still unclear.

Data on the electron dynamics in the TSS are summarized in Fig. 3, where (a) shows snapshots of the 2PPE spectra at selected pump-probe delays Δt. Almost no intensity can be observed for negative delays ($\Delta t = -1$ ps), because we exclusively probe the initially unoccupied states with the chosen probe photon energy. A considerable population of the TSS can be already observed for $\Delta t = 0$ even if the maximum population is reached at $\Delta t \approx 1$ ps. The decay of the populations proceeds on a picosecond time scale. Already from these snapshots it becomes apparent that two energy ranges with different decay dynamics can be distinguished. While the distribution of the population below $E - E_D \approx 150$ meV remains almost unchanged as a function of delay for $\Delta t > 1$ ps and therefore decays with a common decay time, the population at higher energies decays on a faster time scale.

This can be seen in more detail in Fig. 3(c) where the 2PPE intensity within different integration windows as depicted in Fig. 3(b) is plotted as a function of pump-probe delay. The curves for the five lowest energy windows along the TSS are almost identical, whereas the decay becomes faster for higher energy. The red curve shows the intensity within an integration window that is located in the conduction band (CB) at $\bar{\Gamma}$. Obviously, the dynamics is very similar to that of the TSS at the respective energy. This applies for all energies along the TSS and we do not find the sudden increase of the decay rate in the CB just at the CBM as has been reported for $SnSb_2Te_4$ [15]. For increasing energies above E_D, the decay time in the bulk bands (XB) further decreases as indicated by the yellow curve which shows the dynamics at $E - E_D = 650$ meV. Corresponding data for Sb_2Te_2S are presented in Fig. 3(d). They exhibit a very similar behavior.

Figures 3(c) and 3(d) also clearly show that the maximum of the population is not reached during the temporal overlap of pump and probe pulses, but at a much later time. Such delayed filling of the TSS has been also observed in previous 2PPE studies [11,14,15] and has been taken as an evidence for a strong coupling between the TSS and the CB. Our data clearly show that this coupling is also important for Sb_2Te_3 and Sb_2Te_2S. In contrast to the previous 2PPE studies, which all have used pump photon energies around 1.5 eV, however, we observe that the rise of the population in the TSS proceeds on two different time scales. Figures 3(c) and 3(d) clearly show that the initial increase of the 2PPE intensity at $\Delta t = 0$ is very rapid and is followed by a slower increase due to the delayed filling. We attribute the initial faster increase, which accounts for 30%–50% of the total population, to a direct optical excitation of the TSS in Sb_2Te_3 and Sb_2Te_2S with 2.58 eV pump photons.

The decay of the population in the TSS for large delays can be well described by a single-exponential decay [Fig. 3(e)]. Both materials exhibit similar decay times, which are almost constant for low energies and start to decrease at $E - E_D \sim 150$ meV [Fig. 3(f)]. The differences between the two materials are smaller than the variations due to different preparations (dashed lines), which are related to slight variations of $E_D - E_F$. This indicates that the decay is dominated by the number of unoccupied states in the VB as has been concluded for other *p*-doped materials [14,15].

The onset of the decay time decrease is close to the lower edge of the 2PPE signal from the CB of Sb_2Te_3 [see Fig. 1(d)]. For this material, an accelerated decay for higher energies is easy to understand, because one can expect a stronger coupling between TSS and CB if both become degenerated. For Sb_2Te_2S, it is surprising, because we concluded from the 2PPE spectra in agreement with the theory that the CB of Sb_2Te_2S is shifted by ∼100 meV towards higher energies as compared to Sb_2Te_3. Experiments at a lower temperature of 40 K at which the electron mobility in the bulk is enhanced show, however, that the decay times of Sb_2Te_2S become even faster, but only for energies above the onset [open triangles in Fig. 3(f)]. This is a clear indication that the decay of the 2PPE signal at these energies is affected by electron transport into the bulk as has been found for metal and semiconductor surfaces [24–26]. This contradiction might be only solved by performing experiments with different probe photon energies in order to better discriminate between photoemission from bulk and surface states. From the absence of a considerable temperature dependence of the decay times for energies below 150 meV, we conclude that phonons play only a minor role for the decay.

In summary, we have directly accessed the unoccupied electronic structure of *p*-doped Sb_2Te_3 and Sb_2Te_2S with 2PPE, which has unambiguously showed that the massless Dirac-cone-like energy dispersion of the topological surface state is realized for both materials. In agreement with theoretical predictions, we find that the unoccupied bands of Sb_2Te_2S are shifted to higher energies as compared to Sb_2Te_3. The observed electron dynamics strongly indicates that transport perpendicular to the surface is important for the decay in the TSS. Surprisingly, this decay channel becomes operative at the same energy above E_D for both materials. Moreover, our data provide first evidence of a direct optical excitation of the TSS at 2.58-eV photon energy, which might open the possibility to drive a spin current via the circular photogalvanic effect [27]. 2PPE would allow to study its dynamics in unprecedented detail.

We thank H. Bentmann and F. Reinert for providing us Sb_2Te_3 samples and gratefully acknowledge funding by the Deutsche Forschungsgemeinschaft through SPP1666.

[1] M. Z. Hasan and C. L. Kane, Rev. Mod. Phys. **82**, 3045 (2010).

[2] C.-Z. Chang, J. Zhang, X. Feng, J. Shen, Z. Zhang, M. Guo, K. Li, Y. Ou, P. Wei, L.-L. Wang, Z.-Q. Ji, Y. Feng, S. Ji, X. Chen, J. Jia, X. Dai, Z. Fang, S.-C. Zhang, K. He, Y. Wang, L. Lu, X.-C. Ma, and Q.-K. Xue, Science **340**, 167 (2013).

[3] T. V. Menshchikova, S. V. Eremeev, and E. V. Chulkov, JETP Lett. **94**, 106 (2011).

[4] H. Lin, T. Das, L. A. Wray, M. Z. Hasan, and A. Bansil, New J. Phys. **13**, 095005 (2011).

[5] Y. Jiang, Y. Wang, M. Chen, Z. Li, C. Song, K. He, L. Wang, X. Chen, X. Ma, and Q.-K. Xue, Phys. Rev. Lett. **108**, 016401 (2012).

[6] J. Horák, Z. Starý, and J. Klikorka, Phys. Stat. Sol. (b) **147**, 501 (1988).

[7] C. Pauly, G. Bihlmayer, M. Liebmann, M. Grob, A. Georgi, D. Subramaniam, M. R. Scholz, J. Sanchez-Barriga, A. Varykhalov, S. Blugel, O. Rader, and M. Morgenstern, Phys. Rev. B **86**, 235106 (2012).

[8] C. Seibel, H. Maass, M. Ohtaka, S. Fiedler, C. Junger, C. H. Min, H. Bentmann, K. Sakamoto, and F. Reinert, Phys. Rev. B **86**, 161105 (2012).

[9] U. Bovensiepen, H. Petek, and M. Wolf, *Dynamics at Solid State Surfaces and Interfaces: Volume 1 – Current Developments* (Wiley-VCH, Weinheim, 2010).

[10] J. Güdde, M. Rohleder, T. Meier, S. W. Koch, and U. Höfer, Science **318**, 1287 (2007).

[11] J. A. Sobota, S. Yang, J. G. Analytis, Y. L. Chen, I. R. Fisher, P. S. Kirchmann, and Z. X. Shen, Phys. Rev. Lett. **108**, 117403 (2012).

[12] Y. H. Wang, D. Hsieh, E. J. Sie, H. Steinberg, D. R. Gardner, Y. S. Lee, P. Jarillo-Herrero, and N. Gedik, Phys. Rev. Lett. **109**, 127401 (2012).

[13] A. Crepaldi, B. Ressel, F. Cilento, M. Zacchigna, C. Grazioli, H. Berger, P. Bugnon, K. Kern, M. Grioni, and F. Parmigiani, Phys. Rev. B **86**, 205133 (2012).

[14] M. Hajlaoui, E. Papalazarou, J. Mauchain, L. Perfetti, A. Taleb-Ibrahimi, F. Navarin, M. Monteverde, P. Auban-Senzier, C. R. Pasquier, N. Moisan, D. Boschetto, M. Neupane, M. Z. Hasan, T. Durakiewicz, Z. Jiang, Y. Xu, I. Miotkowski, Y. P. Chen, S. Jia, H. W. Ji, R. J. Cava, and M. Marsi, Nat. Commun. **5**, 3003 (2014).

[15] D. Niesner, S. Otto, V. Hermann, T. Fauster, T. V. Menshchikova, S. V. Eremeev, Z. S. Aliev, I. R. Amiraslanov, M. B. Babanly, P. M. Echenique, and E. V. Chulkov, Phys. Rev. B **89**, 081404 (2014).

[16] A. Damm, K. Schubert, J. Güdde, and U. Höfer, Phys. Rev. B **80**, 205425 (2009).

[17] CO exposures up to 10 Langmuir at sample temperatures below 80 K did neither lead to any detectable shift of the Fermi level nor to a change of the electron dynamics in contrast to reports on other compounds [14,15,28,29].

[18] Z.-H. Zhu, C. N. Veenstra, G. Levy, A. Ubaldini, P. Syers, N. P. Butch, J. Paglione, M. W. Haverkort, I. S. Elfimov, and A. Damascelli, Phys. Rev. Lett **110**, 216401 (2013).

[19] M. Bianchi, R. C. Hatch, D. Guan, T. Planke, J. Mi, B. B. Iversen, and P. Hofmann, Semicond. Sci. Technol. **27**, 124001 (2012).

[20] The IPS is excited by the UV pulses and probed by the VIS pulses in both materials. Its natural reference level is the vacuum energy E_{vac}, which is determined by the work function. Within

the experimental uncertainty we find the same work function of 5.0(0.1) eV for both materials from which we determine $E - E_{vac} = 0.85(0.10)$ eV (Sb_2Te_3) and $E - E_{vac} = 0.80(0.10)$ eV (Sb_2Te_2S), respectively.

[21] This value is more than 40% smaller as compared to the value obtained for Sb_2Te_3 thin films by Landau level spectroscopy [5].

[22] S. Souma, K. Eto, M. Nomura, K. Nakayama, T. Sato, T. Takahashi, K. Segawa, and Y. Ando, Phys. Rev. Lett. **108**, 116801 (2012).

[23] S. Muff, F. von Rohr, G. Landolt, B. Slomski, A. Schilling, R. J. Cava, J. Osterwalder, and J. H. Dil, Phys. Rev. B **88**, 035407 (2013).

[24] E. Knoesel, A. Hotzel, and M. Wolf, Phys. Rev. B **57**, 12812 (1998).

[25] S. Tanaka, T. Ichibayashi, and K. Tanimura, Phys. Rev. B **79**, 155313 (2009).

[26] M. Marks, C. H. Schwalb, K. Schubert, J. Güdde, and U. Höfer, Phys. Rev. B **84**, 245402 (2011).

[27] P. Hosur, Phys. Rev. B **83**, 035309 (2011).

[28] D. Hsieh, Y. Xia, D. Qian, L. Wray, J. H. Dil, F. Meier, J. Osterwalder, L. Patthey, J. G. Checkelsky, N. P. Ong, A. V. Fedorov, H. Lin, A. Bansil, D. Grauer, Y. S. Hor, R. J. Cava, and M. Z. Hasan, Nature (London) **460**, 1101 (2009).

[29] M. Bianchi, D. Guan, S. Bao, J. Mi, B. B. Iversen, P. King, and P. Hofmann, Nat. Commun. **1**, 128 (2010).